Low-Cost ZnO-Based Ultraviolet–Infrared Dual-Band Detector Sensitized With PbS Quantum Dots

P. Viraj Vishwakantha Jayaweera, P. K. D. Duleepa P. Pitigala, Jia Feng Shao, Kirthi Tennakone, A. G. Unil Perera, *Senior Member, IEEE*, Pradeep M. Jayaweera, and Jonas Baltrusaitis

***Abstract*—A low-cost photoconductive dual-band detector based on a ZnO film sensitized with lead sulfide quantum dots (PbS-QDs) is reported. The UV response arises from the interband absorption of UV radiation by ZnO, and the *IR* response is due to the absorption in the PbS-QDs. The detector exhibits UV response from 200 to 400 nm with a peak responsivity of 4.0×10^5 V/W and detectivity D^* of 5.5×10^{11} Jones at 370 nm at room temperature. The observed visible–near *IR* response is from 500 to 1400 nm with a responsivity of 5.4×10^5 V/W and D^* of 7.3×10^{11} Jones at 700 nm operating at room temperature. By increasing the PbS-QD size, the *IR* response can extend up to 2.9 μm.**

***Index Terms*—Dual band, lead sulfide quantum dots (PbS-QDs), low cost, ultraviolet–infrared (UV–*IR*), ZnO.**

I. Introduction

A SINGLE detector capable of sensing radiation in two or more distinctly separated spectral regions helps to reduce the cost and size of photon detectors and will be useful for specialized applications such as mine detection and identification of the source of a fire. Several quantum dot (QD), dots-in-well, superlattice, and heterojunction-based dual/multiband detectors have been reported [1], [2]. A typical UV–*IR* dual-band detector uses interband absorption in wide-bandgap nitride semiconductors for UV detection and intraband absorption in the same material for *IR* detection. All of the above detector systems utilize expensive thin-film epitaxial growth techniques such as the molecular beam epitaxy or the metal–organic chemical vapor deposition. On the other hand, nanocrystalline films of wide-bandgap oxide semiconductors, for example, TiO_2, ZnO, and SnO_2, can be fabricated using relatively simple low-cost techniques. These films can be sensitized by semiconductor nanoparticles, such as PbS_3, CdS, Sb_2S_3, and Bi_2S_3 [4].

The electron transport mechanism involved in this type of structures is similar to that in the sensitization of wide-bandgap semiconductors with dyes [5]. The bandgap modulation of QDs due to quantization in particle size enables the sensitization of wide-bandgap materials from UV to far *IR* region [6]. ZnO is an interesting wide-bandgap semiconductor sensitive to the UV radiation, which can be grown by low-cost sol-gel techniques [7], spray pyrolysis, or ducted blading (also known as knife coating) to form nanoporous films. ZnO has several advantages over its competitors, i.e., it is an inexpensive, readily available, chemically stable, and nontoxic material.

Here, a dual-band photoconductive detector, consisting of a ZnO nanoporous film embedded with PbS-QDs, is reported. The UV response originates from the interband absorption of the ZnO with a response threshold corresponding to the bandgap of ZnO at ~ 0.4 μm. The absorption in PbS-QDs leads to a visible to near-*IR* (VIS–NIR) response with a tunable zero-response threshold wavelength λ_t from 0.8 to 2.5 μm. PbS-QDs have a higher bandgap than the bulk PbS (0.41 eV).

There are many reports in the literature describing photoconductive detectors and photovoltaic devices based on PbS-QDs [8]–[10]. The importance of the present system is the observation of enhanced photoconductive response in a disordered composite semiconductor nanostructure.

II. Experimental

Photosensitive films reported here were prepared as described below. A fine diamond point was used to engrave an ~ 30-μm-thick scribe on the surface of a fluorine-doped tin oxide (FTO) conducting glass plate (1×2 cm^2; sheet resistance 12 Ω/sq). After standard cleaning procedures (ultrasonic cleaning in KOH + propan-2-ol followed by rinsing with diluted nitric acid and deionized water and immersion in boiling propan-2-ol), the ZnO paste was screen-printed on top of the area ($\sim 1 \times 1$ cm^2) covering the scribe, as shown in Fig. 1(a).

Manuscript received January 13, 2010; revised July 7, 2010; accepted July 7, 2010. Date of publication August 26, 2010; date of current version September 22, 2010. This work was supported in part by the U.S. National Science Foundation under Grant ECS-0553051, by the U.S. Army Grant W911NF-08-1-0448, and by Georgia Research Alliance Grant GRAUP. The review of this paper was arranged by Editor A. M. Ionescu.

P. V. V. Jayaweera was with the Department of Physics and Astronomy, Georgia State University, Atlanta, GA 30303 USA. He is now with SPD Laboratory Inc., Hamamatsu 432-8003, Japan.

P. K. D. D. P. Pitigala and A. G. U. Perera are with the Department of Physics and Astronomy, Georgia State University, Atlanta, GA 30303 USA (e-mail: uperera@gsu.edu).

J. F. Shao is with the Department of Physics and Astronomy, Georgia State University, Atlanta, GA 30303 USA. He is now with the School of Physical Science and Technology, Lanzhou University, Lanzhou 730000, China.

K. Tennakone is with the Department of Physics and Astronomy, Georgia State University, Atlanta, GA 30303 USA. He is now with the Wayamba University of Sri Lanka, Kuliyapitiya 60200, Sri Lanka.

P. M. Jayaweera is with the Central Microscopy Research Facility, University of Iowa, Iowa City, IA 52242 USA, and also with the Department of Chemistry, University of Sri Jayewardenepura, Nugegoda 10250, Sri Lanka.

J. Baltrusaitis is with the Central Microscopy Research Facility, University of Iowa, Iowa City, IA 52242, USA.

Color versions of one or more of the figures in this paper are available online at http://ieeexplore.ieee.org.

Digital Object Identifier 10.1109/TED.2010.2059631

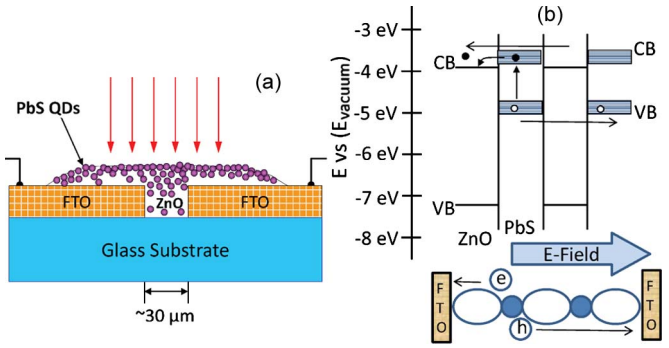

Fig. 1. (a) Schematic illustrating sample geometry used for the dual-band detector. The electrical connectivity of the FTO glass sheet was broken by engraving a scribe, and a layer of colloidal ZnO embedded with PbS-QDs was formed on top. (b) Schematic of approximate conduction and valence-band energy levels in the structure with respect to vacuum scale and possible carrier transport mechanism in the device.

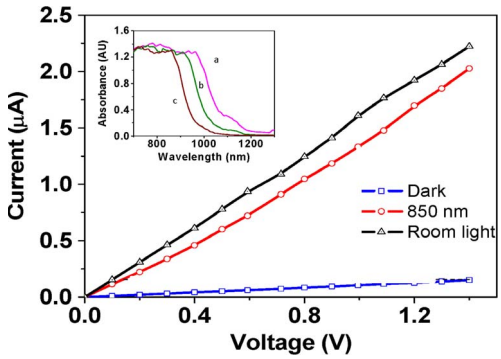

Fig. 2. I–V characteristics of the PbS-coated ZnO sample under dark conditions, and illumination by background light and 850-nm monochromatic radiation with intensity 6.3 μW/cm^2. Linear I–V curves show the ohmic behavior of the detector. (Inset) Shift in the absorption edge with different PbS-QDs on ZnO films [(a), (b), and (c) represent samples S3, S2, and S1, respectively].

The ZnO paste was prepared by grinding 1 g of ZnO powder (Sigma-Aldrich) with some ethanol and a few drops of acetic acid and Triton X-100. Then, the film was dried under ambient conditions and sintered in air at 450 °C for 20 min. The resultant ZnO film was ~10 μm thick. PbS-QDs were embedded on the ZnO film as follows. One drop (~50 μl) of lead (II) acetate ($Pb(CH_3COO)_2 \cdot 3H_2O$) solution in aqueous ethanol was absorbed into the ZnO film and exposed to H_2S gas for 30 min at room temperature. The film acquired a brownish-black tint, which can be observed from both the top and the under side of the ZnO film (through the FTO glass), due to the formation of PbS-QDs. This confirmed the formation of PbS-QDs on the top of the film and also inside the film. By varying the concentration of the lead acetate and the flow rate of H_2S, the density and the size of the PbS-QD particles were altered. Electrical contacts were inserted as shown in Fig. 1(a).

A custom-designed Kratos Axis Ultra X-ray photoelectron spectroscopy (XPS) system [11] was used to obtain the XP spectra of the PbS-QD embedded ZnO film. All XP spectra were calibrated using the adventitious carbon (C) 1 s peak at 285.0 eV. A Shirley-type background was subtracted from each spectrum to account for inelastically scattered electrons that contribute to the broad background. The CasaXPS software was used to process the XPS data [12]. The sulfur 2p transition was fit to two peaks with a ratio of 2 : 1 for the $2p_{3/2}$ and $2p_{1/2}$ transitions, respectively. The sulfur 2p doublet was constrained to have separation energy of 1.2 eV, with equivalent full-width at half-maxima. The components of the peaks contain a Gaussian/Lorentzian product with 30% Lorentzian and 70% Gaussian character. An error of ±0.2 eV is reported for all peak binding energies.

SEM images of FTO glass plates coated with ZnO and ZnO/PbS-QDs, prepared under different H_2S flow rates, were obtained using a Hitachi S-4800 SEM at 2 kV. The I–V characteristics of the samples were measured using a KEITHLEY 2400 source meter. A UV–VIS–NIR monochromator, a lock-in amplifier, and a chopper system with higher order cutoff filters were used to obtain the spectral response. The intensity of the monochromatic light was determined using a calibrated Si and an InGaAs photodiode.

III. Results and Discussion

In smaller PbS-QDs, with a higher bandgap (~1 eV or above), the conduction band (CB) position will be above the CB of the ZnO. Therefore, when VIS–NIR photons are absorbed by PbS-QDs, exited electrons in PbS will be injected into the CB of the ZnO, as shown in the band diagram in Fig. 1(b). With the aid of the external electric field, these carriers (electrons and holes) will drift and tunnel through narrow barriers created by PbS-QDs/ZnO to be collected at the FTO electrodes. On the other hand, for large PbS-QDs, the CB position will be below the CB of ZnO; hence, the electron injection to the CB of ZnO is not possible. Failure to extend the *IR* response to longer wavelengths using a larger PbS-QD is a result of this phenomenon. Therefore, for the device to work, the CB of PbS-QDs has to be above the CB of ZnO.

The current–voltage (I–V) characteristics of the detector under dark ambient room illumination and with a monochromatic illumination (wavelength 850 nm and intensity ~6.3 μW/cm^2) are shown in Fig. 2. Linear I–V curves indicate the ohmic nature of the detector. PbS-QDs improve the conductivity of the ZnO nanocrystalline film owing to filling of pores of the ZnO film with PbS-QDs. The improvement in the conductivity also confirms that PbS-QDs are formed inside the ZnO matrix. Transmission spectra of three different PbS-QD embedded ZnO films, with different-size PbS-QDs, were measured, and the calculated absorbance spectrum is shown in the inset of Fig. 2. These samples were prepared under three different H_2S concentrations, resulting in the formation of different-size PbS-QDs. The sample S1 under a low concentration of H_2S produced smaller QDs, while the sample S3 with a high H_2S concentration produced larger QDs. Transmission measurements were not performed below 320 nm due to the light absorption at wavelengths below 320 nm by the FTO glass.

As shown in Fig. 3, the bare ZnO film gave a response in the range from 200 to 400 nm with a sharp edge at 380 nm, corresponding to the bandgap absorption of ZnO. For comparison, the same ZnO sample was used to embed PbS-QDs. The spectral responsivity of the PbS-QD embedded sample from 200 to 1400 nm at two different bias voltages is also shown in Fig. 3. Responsivities in the UV and NIR regions increased with

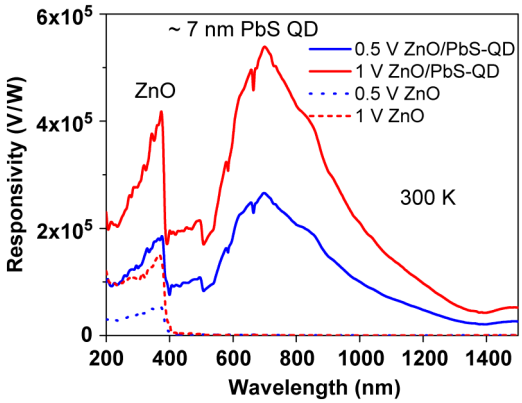

Fig. 3. Responsivity of the PbS-QD embedded ZnO dual-band detector under two different applied biases (0.5 and 1 V) at room temperature. The bottom two curves show the responsivity of the ZnO detector before introducing PbS-QDs. As expected, ZnO shows response only in the UV region with a threshold wavelength at ∼380 nm; this is matched with the bandgap energy of ZnO, 3.3 eV. A load resistor of 2 MΩ was used in all measurements.

the bias voltage up to 1 V (electric field of ∼333 V/cm). It is interesting to note that the presence of PbS-QDs had enhanced the UV responsivity of ZnO by a factor of ∼4. The VIS–NIR response from 500 to 1400 nm with a peak at ∼700 nm clearly shows that the VIS–NIR response is not due to the bulk PbS, which has a bandgap of 0.42 eV (corresponding to λ_t of 2.9 μm). Since the detector is biased in the photoconduction mode, resultant carrier enhancement in the ZnO layer increases the current through the circuit. All the measurements were carried out under ambient conditions.

As illustrated in Fig. 3, the device shows peak responsivities of $\sim 4.0 \times 10^5$ and $\sim 5.4 \times 10^5$ V/W at 380 and 700 nm, respectively. D^* of the devices was calculated from the measured responsivity R_I, noise power density N_d, and the active area of the detector A, i.e.,

$$D^* = \frac{R_I \sqrt{A}}{\sqrt{N_d}} \quad [\text{cm Hz}^{1/2}/\text{W}].$$

N_d of the device at room temperature is $\sim 1.4 \times 10^{-15}$ V^2/Hz, and the active area of the device is 0.003 cm^2. D^* of the device at 380 and 700 nm are 5.5×10^{11} and 7.3×10^{11} Jones, respectively.

SEM images of ZnO and ZnO/PbS-QDs coated plates with two different QD sizes are illustrated in Fig. 4. The ZnO film before deposition of PbS-QDs is shown in Fig. 4(a). Fig. 4(b) and (c) shows ZnO films with PbS-QDs. It can be seen that utilizing low and high concentrations of H_2S has synthesized PbS-QDs of different sizes. The average diameter of the small QDs in Fig. 4(b) is estimated to be 5.0 ± 2 nm, and the PbS-QDs in Fig. 4(c) have an average diameter of 17 ± 3 nm. It was observed that higher concentrations of H_2S could produce much larger QDs. When exposed to very high concentrations of H_2S, these PbS-QDs aggregate to form larger particles with diameters ∼50 nm or larger. These results are in agreement with the absorption spectra of PbS-QDs in polymer films, reported by Wang *et al.* [6], and bandgap energy of PbS-QDs calculated using the finite depth potential model [13]. Using this model and the threshold value of the experimental response spectrum

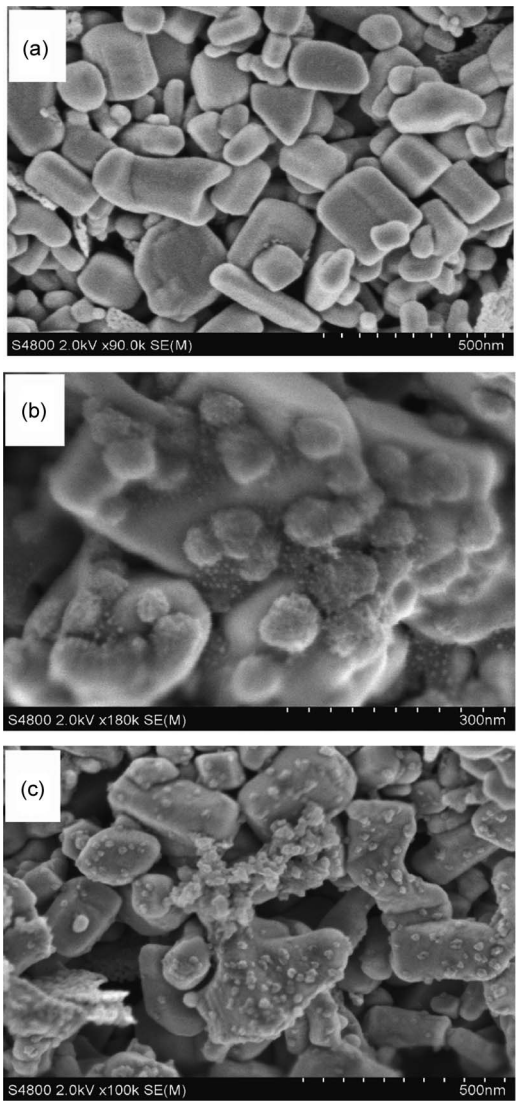

Fig. 4. SEM images of (a) FTO plate coated with ZnO and (b) and (c) FTO plates coated with two different sizes of ZnO/PbS-QDs. The average QD size was estimated as 5.0 ± 2 and 17 ± 3 nm for (b) and (c), respectively.

TABLE I
CALCULATED PHOTORESPONSE THRESHOLD WAVELENGTHS (λ_T) OF THE DETECTORS SENSITIZED WITH DIFFERENT DIAMETER (Φ) OF PbS-QDs

Φ (nm)	λ_T(μm)
7	1.4
10	1.8
20	2.5
30	2.7

(∼1.4 μm), the size of PbS-QDs was calculated as ∼7 nm. Expected threshold wavelengths for different sizes of PbS-QDs are shown in Table I. The work by Guerreiro *et al.* [14], for 6.6-, 7.5-, and 9.8-nm PbS-QDs, confirms experimental absorption thresholds to be close to the theoretical values calculated for 7- and 10-nm PbS-QDs using the model. The weakness of the PbS-induced responsivity in the green region indicates that the percentage of smaller PbS-QDs in the film is relatively small. We have not succeeded in improving the present deposition

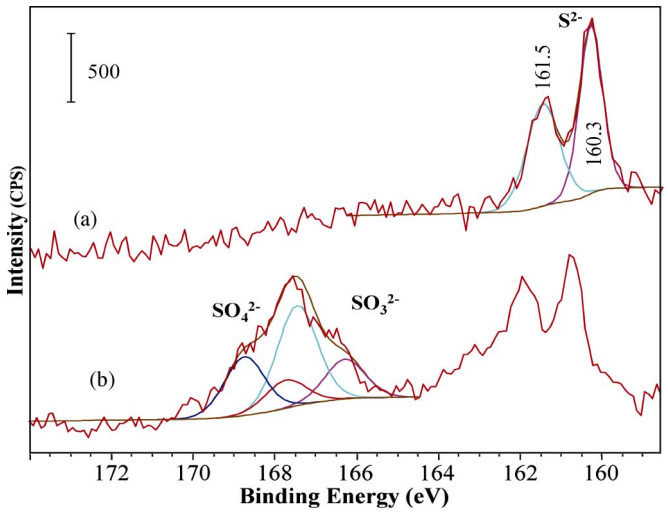

Fig. 5. XPS and peak-fitting curves of the ZnO/PbS-QD sample. (a) Freshly prepared. (b) After exposing the sample to ambient atmospheric conditions for one week.

technique to control the sizes of QDs or to obtain a wider distribution of sizes.

The photoresponse of the device reduced to 10% of its initial value when the sample was stored for one week under ambient conditions. XPS (see Fig. 5) taken at the beginning and after one week indicate oxidation of PbS into $PbSO_4$ and $PbSO_3$. Peak fitting for the SO_3^{2-} species on the surface clearly shows the characteristic binding energies at 165.9 and 167.1 eV. SO_4^{2-} presence is indicated by the characteristic binding energies of 167.5 and 168.7 eV, respectively [see Fig. 5(b)].

Keeping the sample in vacuum eliminated this decaying process. Hence, for practical applications, the detector should be in an airtight sealed package, which can be easily achieved with a polymer sealant. The XPS survey and high-resolution scan spectra of ZnO samples were obtained for comparative studies (not shown here). Upon the deposition of PbS-QDs on ZnO, binding energies of both Zinc-2p and Oxygen-1 s do not show any shift in XPS. Since the XPS is not quite sensitive to detect such interfacial binding energies, covalent bonding of PbS onto the ZnO surface is not ruled out. In ZnO/PbS-QD samples, two XPS peaks appear at 161.5 and 160.3 eV that correspond to the Sulfur-2p region [see Fig. 5(a)]. Scaini *et al.* [15] have reported similar characteristic peaks for vacuum fractured galena samples. These peaks are the result of the Sulfur-$2p_{1/2}$ and Sulfur-$2p_{3/2}$ transitions, respectively [16]. The low binding energies of these two peaks suggest that the sulfur exists as sulfide, i.e., not as either sulfate or sulfite ($PbSO_4$ or $PbSO_3$), which routinely have Sulfur -2p binding energies above 167.0 eV.

Since $Pb(CH_3COOH)_2$ and H_2S were used to make PbS-QDs, it is unlikely to form $Pb(OH)_2$ unless exposed to ambient air for a long time. Nonreacted $Pb(CH_3COOH)_2$ on the surface can be eliminated by exposing the surface to H_2S gas for a fairly long time, particularly with a very dilute $Pb(CH_3COOH)_2$ solution. Furthermore, the appearance of light brownish color confirms the formation of PbS. The XPS, not showing any evidence of having $Pb(OH)_2$ or $Pb(CH_3COOH)_2$ on the film, supports this conclusion. The X-ray diffraction (XRD) spectra did not show any significant difference between the ZnO powder and the PbS-QD embedded ZnO powder. According to literature reports, the XRD peaks of nanocrystalline PbS particles are weak and broad [17].

Although it is not clearly discernable from SEM images, the method of preparation of the film suggests that most voids of the original ZnO film are embedded with PbS nanocrystallites forming at least a partly interconnected network. A Mott–Schottky plot of the film has shown a negative slope indicating the p-type behavior in the film. PbS becomes p-type due to oxygen doping. When these PbS-QDs are photoexcited, minority carriers will be injected into the ZnO (n-type), so electrons and holes will be transported along the ZnO and PbS paths, respectively. Similarly, when the ZnO is excited, holes are injected into the PbS. The above mechanism explains why the ZnO response is enhanced by the PbS.

IV. Conclusion

The low-cost multiband response and easy wavelength tailorability are the advantages of this system. SEM images confirm the different-sized PbS-QD formation on the ZnO film. XPS measurements confirm the formation of PbS and oxidation stability of PbS particles. PbS is transparent to UV radiation, and ZnO is opaque to NIR; therefore, the top region must be sensitive to NIR radiation. The interpenetrating network of p- and n-type materials increases the photoconductivity of the composite system, permitting a current flow under lower biasing voltages. Alternative deposition techniques that improve the filling of voids of the parent film by QDs will increase the responsivity of the system.

References

[1] A. G. U. Perera, "Quantum structures for multiband photon detection," *Opto Electron. Rev.*, vol. 14, no. 2, pp. 99–108, Jun. 2006.

[2] R. C. Jayasinghe, G. Ariyawansa, N. Dietz, A. G. U. Perera, S. G. Matsik, H. B. Yu, I. T. Ferguson, A. Bezinger, S. R. Laframboise, M. Buchanan, and H. C. Liu, "Simultaneous detection of ultraviolet and infrared radiation in a single GaN/GaAlN heterojunction," *Opt. Lett.*, vol. 33, no. 21, pp. 2422–2424, Nov. 2008.

[3] P. Hoyer and R. Konenkamp, "Photoconduction in porous TiO_2 sensitized by PbS quantum dots," *Appl. Phys. Lett.*, vol. 66, no. 3, pp. 349–351, Jan. 1995.

[4] R. Vogel, P. Hoyer, and H. Weller, "Quantum-sized PbS, CdS, Ag2S, Sb_2S_3, and Bi_2S_3 particles as sensitizers for various nanoporous wide-bandgap semiconductors," *J. Phys. Chem.*, vol. 98, pp. 3183–3188, 1994.

[5] M. Grätzel, "Dye-sensitized solar cells," *J. Photochem. Photobiol. C: Photochem. Rev.*, vol. 4, no. 2, pp. 145–153, Oct. 2003.

[6] Y. Wang, A. Suna, W. Mahler, and R. Kasowski, "PbS in polymers. From molecules to bulk solids," *J. Chem. Phys.*, vol. 87, no. 12, pp. 7315–7322, Dec. 1987.

[7] Z.-Q. Xu, H. Deng, J. Xie, Y. Li, and X.-T. Zu, "Ultraviolet photoconductive detector based on Al doped ZnO films prepared by sol-gel method," *Appl. Surf. Sci.*, vol. 253, no. 2, pp. 476–479, Nov. 2006.

[8] G. Konstantatos, I. Howard, A. Fisher, S. Hoogland, J. Clifford, E. Klem, L. Levina, and H. Sargent, "Ultrasensitive solution-cast quantum dot photodetectors," *Nature*, vol. 442, no. 7099, pp. 180–183, Jul. 2006.

[9] K. S. Leschkies, R. Divakar, J. Basu, E. Enache-Pommer, J. E. Boercker, C. B. Carter, U. R. Kortshagen, D. J. Norris, and E. S. Aydil, "Photosensitization of ZnO nanowires with CdSe quantum dots for photovoltaic devices," *Nanoletters*, vol. 7, no. 6, pp. 1793–1798, Jun. 2007.

[10] K. S. Leschkies, T. J. Beatty, M. S. Kang, D. J. Norris, and E. S. Aydil, "Solar cells based on junctions between colloidal PbSe nanocrystals and thin ZnO films," *ACS Nano*, vol. 3, no. 11, pp. 3638–3648, Nov. 2009.

[11] J. Baltrusaitis, C. R. Usher, and V. H. Grassian, "Reactions of sulfur dioxide on calcium carbonate single crystal and particle surfaces at the

adsorbed water carbonate interface," *Phys. Chem. Chem. Phys.*, vol. 9, no. 23, pp. 3011–3024, 2007.
[12] N. Fairley, CasaXPS1999-2008.
[13] Y. Nosaka, "Finite depth spherical well model for excited states of ultrasmall semiconductor particles: An application," *J. Phys. Chem.*, vol. 95, no. 13, pp. 5054–5058, Jun. 1991.
[14] P. T. Guerreiro, S. Ten, F. Borrelli, J. Butty, G. E. Jabbour, and N. Peyghambarian, "PbS quantum-dot doped glasses as saturable absorbers for mode locking of A Cr:forsterite laser," *Appl. Phys. Lett.*, vol. 71, no. 12, pp. 1595–1597, Sep. 1997.
[15] M. J. Scaini, G. M. Bancroft, S. Jsnipe, and W. Geochim, "An XPS, AES, and SEM study of the interactions of gold and silver chloride species with PbS and FeS2: Comparison to natural samples," *Cosmochim. Acta.*, vol. 61, no. 6, pp. 1223–1231, Mar. 1997.
[16] L. Zhang and L. Yang, "A facile method to synthesize spherical PbS and their shape evolution process," *Cryst. Res. Technol.*, vol. 43, no. 10, pp. 1026–1029, Oct. 2008.
[17] N. N. Parvathy, G. M. Pajonk, and A. V. Rao, "Synthesis and study of quantum size effect, XRD and IR spectral properties of PbS nanocrystals doped in SiO2 xerogel matrix," *J. Cryst. Growth*, vol. 179, no. 1/2, pp. 249–257, Aug. 1997.

P. Viraj Vishwakantha Jayaweera received the B.S. degree (Physics Special) from the University of Sri Jayewardenepura, Nugegoda, Sri Lanka, in 1999 and the M.S. and Ph.D. degrees from Georgia State University, Atlanta, in 2007 and 2009, respectively.

He is currently a Senior Scientist with the SPD Laboratory Inc., Hamamatsu, Japan. He has authored or coauthored over 27 technical papers in archival journals. He is the holder of a patent. His research interests include photon detection techniques and development of low-cost photovoltaic cells as a renewable energy source.

Dr. Jayaweera was the recipient of the Outstanding Advanced Graduate Student (Physics) Award in 2007 presented by the Department of Physics, Georgia State University.

P. K. D. Duleepa P. Pitigala received the B.S. degree in physics and the M.Phil. degree from the University of Sri Jayewardenepura, Nugegoda, Sri Lanka, in 2001 and 2008, respectively. He is currently working toward the Ph.D. degree in the Department of Physics and Astronomy, Georgia State University, Atlanta.

He was a Research Assistant with the Institute of Fundamental Studies, Kandy, Sri Lanka, and was an External Student with the Swiss Institute of Technology, Lausanne, Switzerland, in 2007.

Jia Feng Shao received the B.S., M.S., and Ph.D. degrees from Lanzhou University, Lanzhou, China, in 1994, 1997, and 2010, respectively.

He is currently a Teacher with the School of Physical Science and Technology, Lanzhou University.

Dr. Shao was the recipient of the "Excellent Young Teacher" from Lanzhou University in 2002.

Kirthi Tennakone received the Ph.D. degree in theoretical physics from the University of Hawaii, Honolulu, in 1972.

He was a Professor of physics with the University of Ruhuna, Matara, Sri Lanka, and a Research Professor, the holder of the endowed Sumanasekara Chair in Natural Science, and the Director of the Institute of Fundamental Studies, Kandy, Sri Lanka. He is currently an Honorary Research Professor with Wayamba University of Sri Lanka, Kuliyapitiya, Sri Lanka. His research interests include many areas of theoretical and experimental physics and physical chemistry. His current research activity is focused mainly on experimental and theoretical materials science related to solar energy conversion, optoelectronic device physics, and dielectrics.

A. G. Unil Perera (SM'03) received the B.S. degree in physics (with first class honors) from the University of Colombo, Colombo, Sri Lanka, and the M.S. and Ph.D. degrees from the University of Pittsburgh, Pittsburgh, PA.

He is currently the Associate Chair of the Department of Physics and Astronomy and the Graduate Director of the Physics Program with the Georgia State University, Atlanta. His focus is on developing multiband and terahertz photon detectors. He has participated in several "advanced research workshops" and has presented invited talks at many conferences. He has written six book chapters, contributed to the CRC dictionary of electronics, and coedited a volume on thin-film optical devices for a five-volume handbook. He has served on the National Science Foundation, Department of Energy, and National Aeronautics and Space Administration review panels and also as a reviewer for numerous research proposals and papers. He has had over 130 technical articles published. He is the holder of five patents (or applications). His work was featured in various professional journals such as *Laser Focus World*, *Photonics Spectra*, and the *Reviews of Modern Physics*.

Dr. Perera is a Fellow of the American Physical Society and the Society of Photo-Instrumentation Engineers.

Pradeep M. Jayaweera received the B.S. degree from the University of Sri Jayewardenepura, Nugegoda, Sri Lanka, in 1991 and the Ph.D. degree from the Queen's University of Belfast, Belfast, Northern Ireland, in 1996.

He is currently a Professor with the Department of Chemistry, University of Sri Jayewardenepura, Nugegoda, Sri Lanka. His main research interests involve solar energy conversion, Raman, surface-enhanced Raman, excited-state properties of metal complexes, and surface chemistry of nanoparticles.

Jonas Baltrusaitis was born in Lithuania. He received the B.S. degree in chemical engineering in 1998 and the Ph.D. degree in chemistry from the University of Iowa, Iowa City, in 2007.

He is currently an Assistant Research Scientist with the Central Microscopy Research Facility, University of Iowa. His research interests involve surface chemistry, electron spectroscopy and microscopy, heterogeneous catalysis, and photocatalysis of carbon dioxide.